MIT Libraries | DSpace@MIT

MIT Open Access Articles

Lyapunov spectrum of scale-resolving turbulent simulations. Application to chaotic adjoints

The MIT Faculty has made this article openly available. ***Please share*** how this access benefits you. Your story matters.

Citation: Fernandez, Pablo, and Qiqi Wang. "Lyapunov Spectrum of Scale-Resolving Turbulent Simulations. Application to Chaotic Adjoints." 23rd AIAA Computational Fluid Dynamics Conference (June 2, 2017), Denver, Colorado, 2017.

As Published: https://doi.org/10.2514/6.2017-3797

Publisher: American Institute of Aeronautics and Astronautics (AIAA)

Persistent URL: http://hdl.handle.net/1721.1/115070

Version: Author's final manuscript: final author's manuscript post peer review, without publisher's formatting or copy editing

Terms of use: Creative Commons Attribution-Noncommercial-Share Alike

Massachusetts Institute of Technology

Lyapunov spectrum of chaotic flow simulations. Application to chaotic adjoints

P. Fernandez*, Q. Wang†

Massachusetts Institute of Technology, Cambridge, MA 02139, United States

We present an investigation of the Lyapunov spectrum of the chaotic, separated flow around the NACA 0012 airfoil at Reynolds number 2,400. The impact of the numerical discretization on the spectrum is investigated through time and space refinement studies. Numerical results show that the time discretization has a small impact on the Lyapunov exponents, whereas the spatial discretization can dramatically change them. In particular, the asymptotic Lyapunov spectrum for this wall-bounded flow is achieved with global CFL numbers as large as $\mathcal{O}(10^1 - 10^2)$, whereas the system continues to become more and more chaotic as the mesh is refined even for meshes that are much finer than the best practice for this type of flows. Based on these results, we conclude the paper with a discussion on the feasibility of adjoint-based sensitivity analysis for chaotic flows.

I. Introduction

With the increase in computing power, scale-resolving turbulence simulations, such as large-eddy simulation (LES) and direct numerical simulation (DNS), emerge as promising approaches to improve both knowledge of complex flow physics and reliability of flow predictions. While these techniques have become essential tools in flow physics, no comparable impact has been observed in engineering. The chaotic dynamics that these simulations inherit from the underlying turbulent flow are largely responsible for this lag. First, the chaotic and multiscale nature of turbulent flows make numerical simulation of turbulence computationally demanding. Second, conventional sensitivity analysis methods break down for chaotic systems;[14] which compromises critical tasks in engineering such as flow control, design optimization, error estimation, data assimilation, and uncertainty quantification. While a number of sensitivity analysis methods have been proposed for chaotic systems, including Fokker-Planck methods,[23] Fluctuation-Dissipation methods,[15] the Ensemble Adjoint (EA) method,[14] the Least Squares Shadowing (LSS) method[26] and the Non-Intrusive Least Squares Shadowing (NILSS) method,[17] they all come at a high computational cost. This is ultimately related to the positive portion of the Lyapunov spectrum of the system, and the cost of each method is sensitive to different aspects of it. For example, the cost of NILSS is, by construction, proportional to the number of positive exponents,[17] whereas the cost of EA is postulated to depend on the largest Lyapunov exponent and the rate of decay of correlations in the chaotic system.[5,6] Understanding the Lyapunov spectrum of chaotic flow simulations and its dependence on numerical discretization is therefore necessary to estimate the cost and feasibility of chaotic sensitivity analysis methods, drive strategic decisions about those with the most promise, and provide insight to devise superior methods.

Lyapunov analysis is also an important tool in flow physics. With the first attempts to apply these techniques to chaotic fluid flows dating back from the '90s,[13,20,21] Lyapunov analysis currently gains attention in the flow physics community for flow instability, vortex dynamics and turbulence research.[4,16,24,25,27,28] While the interest in flow physics lies in the Lyapunov spectrum of the actual flow, numerical algorithms compute the Lyapunov exponents of the finite-dimensional representation obtained after numerical discretization. Before these techniques become routine in the community and more publications appear, it is critical to understand the role of the spatial and temporal discretization on the resulting dynamics: Is the spectrum of the discrete system that of the actual flow? If so, how much resolution is required to reproduce the true dynamics? That is, how much resolution is required for these studies to be reliable and trustworthy?

In this paper, we investigate the impact of numerical discretization on the Lyapunov spectrum of the two-dimensional, separated flow around the NACA 0012 airfoil at Reynolds number $Re_\infty = 2,400$, Mach number $M_\infty = 0.2$, and

*PhD Student, Department of Aeronautics and Astronautics, MIT, AIAA Student Member. Email: pablof@mit.edu

†Associate Professor, Department of Aeronautics and Astronautics, MIT, AIAA Member. Email: qiqi@mit.edu

angle of attack $\alpha = 20$ deg. Since the simulation is two-dimensional, the flow physics are different to those of three-dimensional flows. However, the moderate computational cost of this problem allows for a more comprehensive study than otherwise possible. In particular, the impact of the temporal resolution (t-refinement) and spatial resolution (h-refinement) are investigated. More importantly, this two-dimensional study suffices for our purpose here. First, it provides insight on the feasibility of sensivitiy analysis for chaotic flows. Second, it illustrates some potential limitations of Lyapunov analysis for flow physics applications. For an extension of the results and the discussions in this work, the interested reader is referred to.[11]

The remainder of the paper is organized as follows. In Section II, we present an overview of Lyapunov analysis. Section III describes the methodology to discretize the Navier-Stokes equations and compute Lyapunov exponents. Numerical results are then presented in Section IV. Based on these results, we discuss the feasibility of sensitivity analysis for chaotic flows in Section V. Finally, some concluding remarks are presented in Section VI.

II. Lyapunov analysis

The spatial discretization of the compressible Navier-Stokes equations for a Newtonian fluid yields an autonomous, continuous-time, first-order dynamical system of the form

$$\frac{d\boldsymbol{u}_h}{dt} = \boldsymbol{f}_h(\boldsymbol{u}_h), \tag{1}$$

where $\boldsymbol{u}_h = \boldsymbol{u}_h(t)$ is an n-dimensional vector of state variables. In particular, $\boldsymbol{u}_h$ contains the conserved quantities (mass, momentum and total energy) at every grid point. Different meshes h and numerical schemes lead to different dimensions n and different dynamics $\boldsymbol{f}_h$.

For an ergodic system of the form (1), almost surely there exist scalars $\Lambda_h^1, \Lambda_h^2, ..., \Lambda_h^n \in \mathbb{R}$ such that, if $\Lambda_h^1 \neq \Lambda_h^2 \neq ... \neq \Lambda_h^n$, there exist vectors $\boldsymbol{\psi}_h^1(\boldsymbol{u}_h), \boldsymbol{\psi}_h^2(\boldsymbol{u}_h), ..., \boldsymbol{\psi}_h^n(\boldsymbol{u}_h) \in \mathbb{R}^n$ satisfying the evolution equation[19]

$$\frac{d}{dt}\boldsymbol{\psi}_h^j\big(\boldsymbol{u}_h(t)\big) = \left.\frac{\partial \boldsymbol{f}_h}{\partial \boldsymbol{u}_h}\right|_{\boldsymbol{u}_h(t)} \boldsymbol{\psi}_h^j\big(\boldsymbol{u}_h(t)\big) - \Lambda_h^j\, \boldsymbol{\psi}_h^j\big(\boldsymbol{u}_h(t)\big), \quad j = 1, ..., n. \tag{2}$$

$\boldsymbol{\psi}_h^j(\boldsymbol{u}_h)$ and Λ_h^j are the so-called covariant Lyapunov vectors (CLVs) and Lyapunov exponents (LEs), respectively. Again under ergodicity assumptions, the CLVs depend on the state $\boldsymbol{u}_h$, whereas the LEs are a property of the system independent of $\boldsymbol{u}_h$. Also, we shall asume that the Lyapunov exponents $\Lambda_h^1, ..., \Lambda_h^n$ are ordered from largest to smallest.

The intuitive interpretation of Lyapunov vectors and exponents is as follows: "Any infinitesimal perturbation $\delta\boldsymbol{u}_{h,0}$ in the direction $\boldsymbol{\psi}_h^j\big(\boldsymbol{u}(t_0)\big)$ at $t = t_0$ will remain in $\boldsymbol{\psi}_h^j\big(\boldsymbol{u}_h(t)\big)$ at all times $t \geq t_0$. Also, the magnitude of the perturbation increases or decreases at an average rate $\delta u_h(t) = \delta u_{h,0}\ \exp\big(\Lambda_h^j(t - t_0)\big)$". Hence, the magnitude and sign of the Lyapunov exponents characterize how infinitesimal perturbations to the system evolve over time. In particular, a system with $n^+ \geq 1$ positive exponents, $\Lambda_h^+ = \{\Lambda_h^1, ..., \Lambda_h^{n_+}\}$, displays chaotic dynamics. The positive exponent(s) are responsible for the "butterfly effect", a colloquial term to refer to the large sensitivity of chaotic systems to initial conditions. Turbulent flows, as well as many separated flows, are examples of chaotic systems.

The numerical simulation of unsteady flows requires further discretizing Eq. (1) in time. This yields an autonomous, discrete-time, first-order map

$$\boldsymbol{u}_h^{(i+1)} = \boldsymbol{f}_{h,\Delta t}(\boldsymbol{u}_h^{(i)}), \tag{3}$$

where $\boldsymbol{u}_h^{(i)}$ denotes the solution at the end of the time step i. The particular form of $\boldsymbol{f}_{h,\Delta t}$ depends on $\boldsymbol{f}_h$ (i.e. on the spatial discretization), as well as on the time-integration scheme and the time-step size Δt. The discrete-time Lyapunov vectors $\boldsymbol{\psi}_{h,\Delta t}^j$ and exponents $\Lambda_{h,\Delta t}^j$ of $\boldsymbol{f}_{h,\Delta t}$ are defined in an analogous way to their continuous counterparts.

III. Methodology

A. Numerical discretization

High-order Hybridizable Discontinuous Galerkin (HDG) and diagonally implicit Runge-Kutta (DIRK) methods are used for the spatial and temporal discretization of the compressible Navier-Stokes equations, respectively.[10] The DIRK scheme, as an L-stable time-integration scheme, allows for a systematic study of the effect of the time-step size without running into numerical stability issues. A detailed description of the numerical discretization and the parallel iterative solver can be found in.[8–10]

B. LE algorithm

A non-intrusive version of the algorithm by Benettin *et al.*[1] is used to compute the p ($\leq n$) leading Lyapunov exponents.

Original algorithm. The original method in[1] is summarized in Algorithm 1. If the time integrals in Steps No. 5 and 6 of the algorithm are computed exactly, an estimator of the p leading continuous-time LEs $\hat{\Lambda}_h$ of $\boldsymbol{f}_h$ are obtained. If the time integrals are approximated using a numerical method, as it is the case in practice, the algorithm computes an estimator of the p leading discrete-time Lyapunov exponents $\hat{\Lambda}_{h,\Delta t}$ of $\boldsymbol{f}_{h,\Delta t}$. Also, the time segment T_s needs to be such that $T_s \Lambda_h^1 \ll \epsilon_m^{-1}$ in order to ensure the numerically stability of the iteration, where ϵ_m denotes machine epsilon.

Data: Initial condition $\boldsymbol{u}_{h,0}$, number of exponents to compute p, length of each time segment T_s, and number of time segments K.
Result: Estimators of the p largest LEs $\hat{\Lambda}_h^j,\ j = 1, ..., p$.
1. Set $t_0 = 0$ and $\boldsymbol{u}_h(t_0) = \boldsymbol{u}_{h,0}$.
2. Compute an $n \times p$ random matrix

$$V^{\langle 0 \rangle} \sim \left[\mathcal{U}(0,1)\right]^{n \times p},$$

where $\mathcal{U}$ denotes the continuous uniform distribution.
3. Compute the reduced QR decomposition

$$Q^{\langle 0 \rangle} R^{\langle 0 \rangle} = V^{\langle 0 \rangle}.$$

for $i = 1$ **to** K **do**
4. Set $t_i = t_{i-1} + T_s$.
5. Time integrate the dynamical system (1) from t_{i-1} to t_i using the initial condition $\boldsymbol{u}_h^{\langle i-1 \rangle} = \boldsymbol{u}_h(t_{i-1})$.
6. Time integrate the tangent equation (4) from t_{i-1} to t_i for each of the p initial conditions given by the columns of $Q^{\langle i-1 \rangle}$ using the reference trajectory $\boldsymbol{u}_h$ computed in Step No. 5,

$$\frac{d\boldsymbol{v}_j}{dt} = \left.\frac{\partial \boldsymbol{f}_h}{\partial \boldsymbol{u}_h}\right|_{\boldsymbol{u}_h(t)} \boldsymbol{v}_j, \qquad \boldsymbol{v}_j(t_{i-1}) = \boldsymbol{q}_j^{\langle i-1 \rangle}, \tag{4}$$

for $j = 1, ..., p$, and set $\boldsymbol{v}_j^{\langle i \rangle} = \boldsymbol{v}_j(t_i)$. Here, $\boldsymbol{q}_j^{\langle i \rangle}$ and $\boldsymbol{v}_j^{\langle i \rangle}$ denote the j-th column of $Q^{\langle i \rangle}$ and $V^{\langle i \rangle}$.
7. Compute the reduced QR decomposition

$$Q^{\langle i \rangle} R^{\langle i \rangle} = V^{\langle i \rangle}.$$

end
8. Compute

$$\hat{\Lambda}_h^j = \frac{1}{t_K - t_0} \sum_{i=1}^{K} \log |R_{jj}^{\langle i \rangle}|. \tag{5}$$

Algorithm 1: Original algorithm by Benettin *et al.*[1] to compute LEs. The superscript $\langle i \rangle$ denotes the solution at the end of the time segment i.

Modified algorithm. Since the original algorithm requires the integration of the homogeneous tangent equation (4) in Step No. 6, it cannot be used with most existing computational fluid dynamics (CFD) solvers without modification of the source code. In the spirit of making the algorithm non-intrusive, we approximate the tangent map (4) by finite differences. In particular, let $\boldsymbol{u}_h^{\langle i \rangle} = \boldsymbol{g}_{h,\Delta t}(\boldsymbol{u}_h^{\langle i-1 \rangle};\ T_s)$ denote the Navier-Stokes map over a time segment of length T_s computed by a CFD code starting from the initial condition $\boldsymbol{u}_h^{\langle i-1 \rangle}$. We then replace Step No. 6 in Algorithm 1 by

$$\boldsymbol{v}_j^{\langle i \rangle} \approx \frac{1}{\epsilon}\Big[\boldsymbol{g}_{h,\Delta t}\big(\boldsymbol{u}_h(t_{i-1}) + \epsilon\, \boldsymbol{q}_j^{\langle i-1 \rangle};\ T_s\big) - \boldsymbol{g}_{h,\Delta t}\big(\boldsymbol{u}_h(t_{i-1});\ T_s\big)\Big], \tag{6}$$

for $j = 1, ..., p$. The use of a forward finite difference approximation (FFDA) for the tangent field introduces some restrictions on T_s and ϵ. First, while the tangent field diverges exponentially and is unbounded for chaotic flows, $||\boldsymbol{g}_{h,\Delta t}||$ is bounded above for all T_s. Hence, the length of the time segments must be small enough so that the

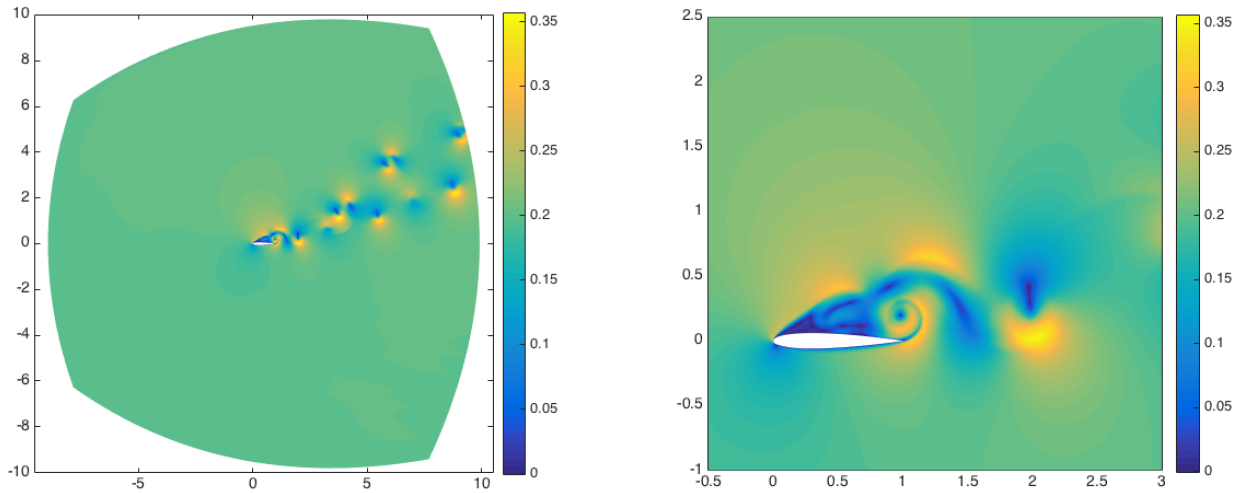

Figure 1: Snapshot of Mach number field.

perturbation lies within the linear region, i.e.

$$||\boldsymbol{g}_{h,\Delta t}\big(\boldsymbol{u}_h(t_{i-1}) + \epsilon\, \boldsymbol{q}_j^{\langle i-1\rangle};\, T_s\big) - \boldsymbol{g}_{h,\Delta t}\big(\boldsymbol{u}_h(t_{i-1});\, T_s\big)|| \ll ||\boldsymbol{g}_{h,\Delta t}\big(\boldsymbol{u}_h(t_{i-1});\, T_s\big)||, \tag{7}$$

and the FFDA provides an accurate representation of the tangent field. Second, ϵ must satisfy $\epsilon_m \ll \epsilon \ll ||\boldsymbol{u}_h||$. Third, the use of an implicit time integration scheme requires $\epsilon_{tol} \ll ||\partial \boldsymbol{f}_{h,\Delta t}/\partial \boldsymbol{u}_h||\, \epsilon$, where ϵ_{tol} is the tolerance the nonlinear system arising from the time discretization is solved to.

IV. Numerical results

A. Case description

We consider the two-dimensional, separated flow around the NACA 0012 airfoil at Reynolds number $Re_\infty = u_\infty c/\nu = 2400$, Mach number $M_\infty = u_\infty/a_\infty = 0.2$, and angle of attack $\alpha = 20$ deg. Here, u_∞, a_∞, ν, and c denote the freestream velocity, freestream speed of sound, kinematic viscosity and airfoil chord, respectively. The computational domain is partitioned using isoparametric triangular c-meshes, and the outer boundary is located 10 chords away from the airfoil. A non-slip, adiabatic wall boundary condition is imposed on the airfoil surface, and a characteristics-based, non-reflecting boundary condition is used on the outer boundary. A run up time $t_0 = 2,000\ c/a_\infty$ is used to drive the system to the attractor, and the LE algorithm is then applied for $K = 12,000$ time segments, each of length $T_s = c/a_\infty$. A snapshot of the Mach number field for this flow is shown in Fig. 1.

B. Effect of time resolution: t-refinement study

We analyze the effect of the time-step size on the Lyapunov spectrum of the discrete system $\boldsymbol{f}_{h,\Delta t}$. In particular, the continuous-time system $\boldsymbol{f}_h$ associated to a fourth-order HDG discretization with 115,200 degrees of freedom (DOFs) is time-integrated using a third-order DIRK method with time steps $\Delta t = (0.20,\ 0.10,\ 0.05,\ 0.025,\ 0.0125)\ c/a_\infty$. These correspond to global CFL numbers $\Delta t\ u_\infty/h_{min}$ of 59.94, 29.97, 14.98, 7.49, and 3.75, where h_{min} denotes the smallest element size in the mesh. We emphasize that the time-step size affects the discrete-time map $\boldsymbol{f}_{h,\Delta t}$ but it does not change $\boldsymbol{f}_h$.

Figure 2 shows 90% confidence intervals of the six leading Lyapunov exponents for the time-step sizes considered. From this figure, the time-step size in the range considered does not have a significant impact on the leading exponents of $\boldsymbol{f}_{h,\Delta t}$. First, this gives us confidence that the discrete-time Lyapunov exponents approximate those of the continuous-time system, i.e. $\Lambda^j_{h,\Delta t} \approx \Lambda^j_h$. This indicates that these time steps suffice to resolve all the vortical structures that are responsible for the chaotic dynamics of $\boldsymbol{f}_h$. For this reason, we shall refer to $\boldsymbol{f}_h$ and Λ^j_h instead of $\boldsymbol{f}_{h,\Delta t}$ and $\Lambda^j_{h,\Delta t}$ in the remainder of the paper. Second, the asymptotic spectrum of the discrete-time map as $\Delta t \downarrow 0$ is achieved with global CFL numbers $\mathcal{O}(10-100)$ that are much larger than those used in engineering practice. The

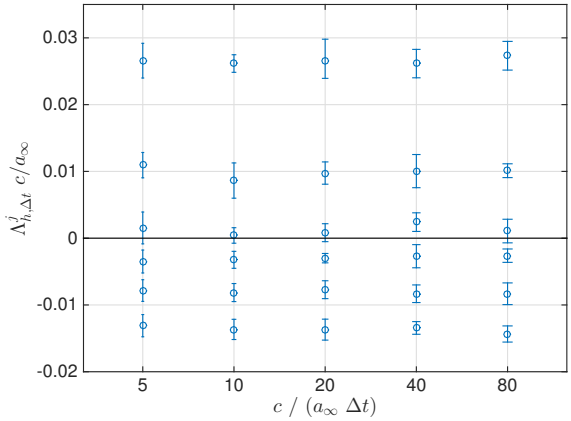

Figure 2: 90% confidence intervals of the six leading Lyapunov exponents in the t-refinement study.

accurate prediction of the Lyapunov spectrum with such large CFL numbers is attributed to the smallest element size (near the leading edge, where the flow is laminar) being much smaller than the element sizes in the separated region of the flow. However, if the time step was larger than $\tilde{h}/u_\infty$, where $\tilde{h}$ denotes the smallest length scale responsible for chaos in the continuous-time system, the discrete-time map might not accurately reproduce the continuous-time map and thus $\Lambda^j_{h,\Delta t} \not\approx \Lambda^j_h$. A similar observation has been reported in[18] for the numerical integration of stiff ODEs with inadequate time steps.

C. Effect of spatial resolution: h-refinement study

In this section, we examine the effect of the spatial resolution on the number and magnitude of positive exponents. To that end, the Lyapunov spectrum of the flow is computed with eleven meshes, each of them $2^{1/3}$ times finer per direction than the previous one. The number of DOFs uniformly increases in logarithmic scale from 7,200 (mesh No. 1) to 726,240 (mesh No. 11). Meshes No. 1 and 11 are shown in Fig. 3. We note that mesh No. 1 is intended to be pathologically coarse to analyze how the system behaves for very under-resolved simulations.

The discretization scheme and time-step size are kept constant to analyze the effect of spatial resolution only. Again, fourth-order HDG and third-order DIRK methods are used for the spatial and temporal discretization, respectively, and the time-step size is set to $\Delta t = 0.05\ c/a_\infty$. Figure 4 shows the 14 leading LEs for the discretizations considered. From these results, several remarks follow:

- The magnitude of the leading LE and the number of positive exponents increase above some spatial resolution threshold h^*, corresponding to mesh No. 5 here. That is, the discrete system becomes more chaotic above this resolution as the mesh is refined. This is attributed to the fact that more vortical structures, which are responsible for the chaotic dynamics of the flow, are resolved as the numerical resolution is increased.

- Below the resolution threshold h^*, the discrete system poorly reproduces the dynamics of the continuous system, and this results in spurious dynamics. Here, spurious periodicity and chaoticity are observed. (No discretization results in stable dynamics.) Discretization No. 5, for example, has no positive LEs and is periodic. A time refinement study confirmed that the continuous-time system associated to this discretization $\boldsymbol{f}_{h_5}$ –and not only the discrete-time map $\boldsymbol{f}_{h_5,\Delta t}$– is indeed periodic. Hence, for the h-family of discrete dynamical systems considered here, a periodic orbit bifurcates into strange attractors above and below $h^* \approx h_5$.

  We hypothesize this is a numerical artifact and therefore discretization dependent. For example, spurious chaoticity may not be observed in methods with high numerical dissipation, such as first-order schemes. For these methods, very coarse meshes may result instead in stable dynamics with a fixed point.

- An approximately zero exponent $\Lambda_h \approx 0$ is present in all discretizations. Theoretical results show that at least one neutrally stable Lyapunov exponent $\Lambda_h = 0$ exists for periodic and chaotic systems[12] and that $\boldsymbol{\psi}_h = \boldsymbol{f}_h(\boldsymbol{u}_h)$ is a CLV for this exponent. This is expected to be such an LE and the error is attributed to the variance of the estimator.

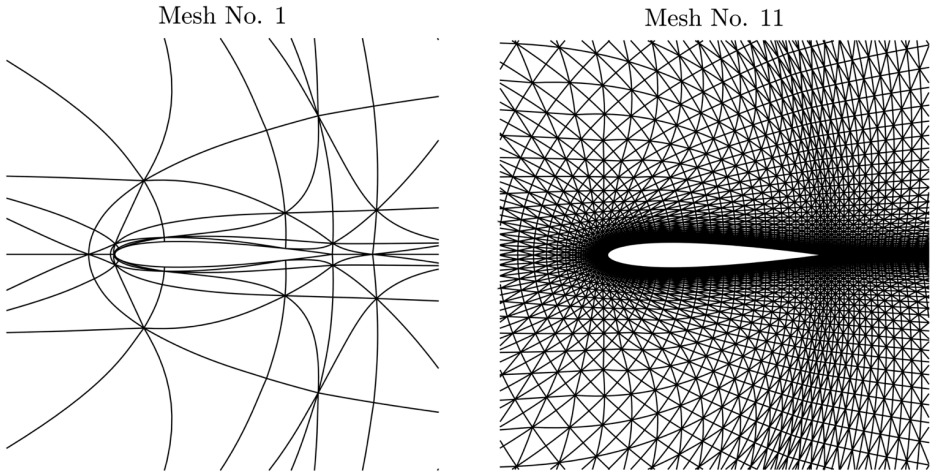

Figure 3: Coarsest and finest high-order meshes used in the h-refinement study.

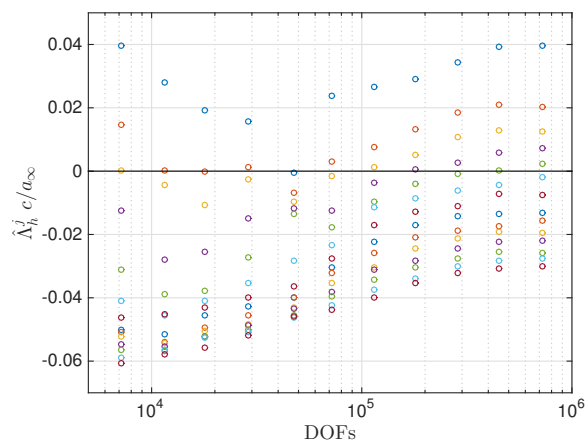

Figure 4: 14 leading Lyapunov exponents of the h-family of dynamical systems.

- The positive Lyapunov exponents are created from bifurcations of the $\Lambda_h = 0$ exponent at discrete mesh resolutions. This provides insight on the mechanisms responsible for the increase of chaoticity as the mesh is refined.

The discrete Fourier transform (DFT) of the lift coefficient, drag coefficient and static pressure at the trailing edge for the discretizations No. 5 and 7 are displayed in Fig. 5. The trace of drag vs. lift coefficients over a time interval of length $20,000 \; c/a_\infty$ is shown in Fig. 6, where the dots are colored by probability density function (PDF) in (c_d, c_l) space. Despite the chaotic dynamics of discretization No. 7, its PDF resembles the periodic trace of mesh No. 5.

Next, we investigate if an asymptotic Lyapunov spectrum is achieved with the numerical resolutions that can be afforded in engineering practice. To this end, we consider a fourth-order discretization with 2,880,000 degrees of freedom; which is vastly more than the best-practice meshes for this type of flows. The 90% confidence interval of the leading Lyapunov exponent for this discretization is $\Lambda_h^1 \; c/a_\infty = 0.04732 \pm 0.005275$. Hence, the system becomes more chaotic even for this discretization. While an asymptotic Lyapunov spectrum as $h \downarrow 0$ was obtained for simpler partial differential equations in other studies,[22] this shows that such an asymptotic spectrum –if exists– is difficult to achieve in practice even for simple flows and cannot be obtained with the resolutions used in engineering practice. This is in contrast to the results for the time discretization in Section B.

We conjecture that an asymptotic Lyapunov spectrum does indeed exist and that the leading exponent is inversely proportional to the smallest time scales responsible for chaos. Therefore, the mesh size required to accurately compute the Lyapunov spectrum may need to be of the order of the smallest chaotic length scale. In the case of turbulent flows,

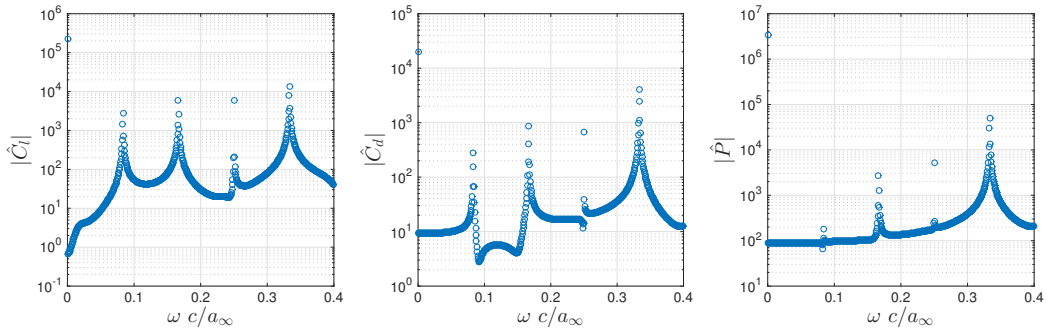

(a) Mesh No. 5

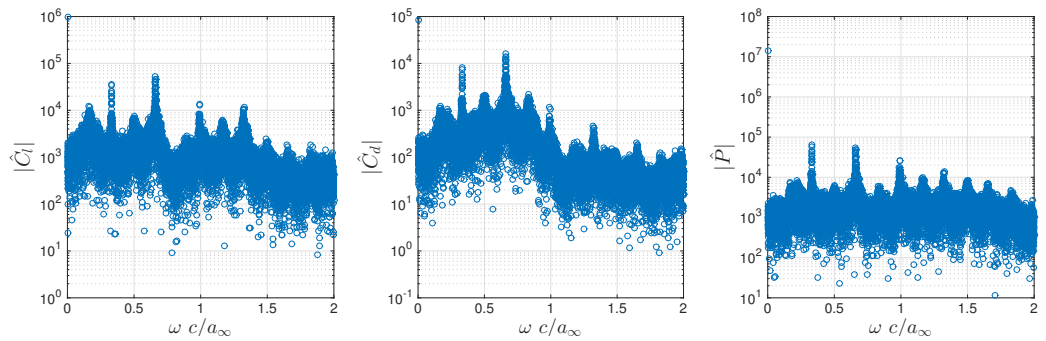

(b) Mesh No. 7

Figure 5: Discrete Fourier transform of lift coefficient, drag coefficient and pressure at the trailing edge for discretizations No. 5 (top) and 7 (bottom).

this corresponds to DNS resolutions and is consistent with the results in.[16]

V. Application to chaotic adjoints

We conclude with a discussion on the implications of the numerical results in this paper on adjoint-based sensitivity analysis for chaotic flows. On the one hand, the discrete system being less chaotic than the actual flow makes sensitivity analysis more manageable. In particular, the cost of the two main adjoint-based sensitivity methods in the literature, namely the Least Squares Shadowing (LSS)[26] and the Ensemble Adjoint (EA) methods, increases with the number and/or magnitude of positive Lyapunov exponents in the discrete system. The computational cost of shadowing-based approaches, including the original LSS method, the Multiple Shooting Shadowing (MSS) method[2] and the Non-Intrusive LSS (NILSS) method,[3,17] is proportional to the number of positive Lyapunov exponents. Under optimistic assumptions, including uniform hyperbolicity and exponential decay of correlations, Chandramoorthy *et al.*[5,6] showed that the mean squared error in the EA estimator is a power law of the computational cost, where the power constant depends on the leading exponent. From the numerical results in this paper and related studies on the Lyapunov spectrum of turbulent flows,[4,6] the cost of the EA method is expected to remain prohibitive for most industrial applications for a number of years. This is due to the variance of the EA estimator diverging exponentially at a rate that is related to the leading Lyapunov exponent. Shadowing-based methods, however, and in particular an accelerated version of NILSS currently under investigation, may enable sensitivity analysis of turbulent flows in the near future. This is due to the variance of the shadowing estimator not diverging exponentially; which comes at a cost that is only linear on the number of positive exponents.

On the other hand, the discrete system being less chaotic than the actual flow may raise questions on the accuracy of the computed sensitivities. In this regard, we note that most quantities of interest in engineering applications require only an accurate description of the large scales in the turbulent flow, that is, LES-type resolutions. The numerical results in this paper, however, indicate that accurately computing the Lyapunov spectrum requires resolving all the length and time scales responsible for chaos, that is, DNS-type resolutions. As a result, accurate sensitivities may be

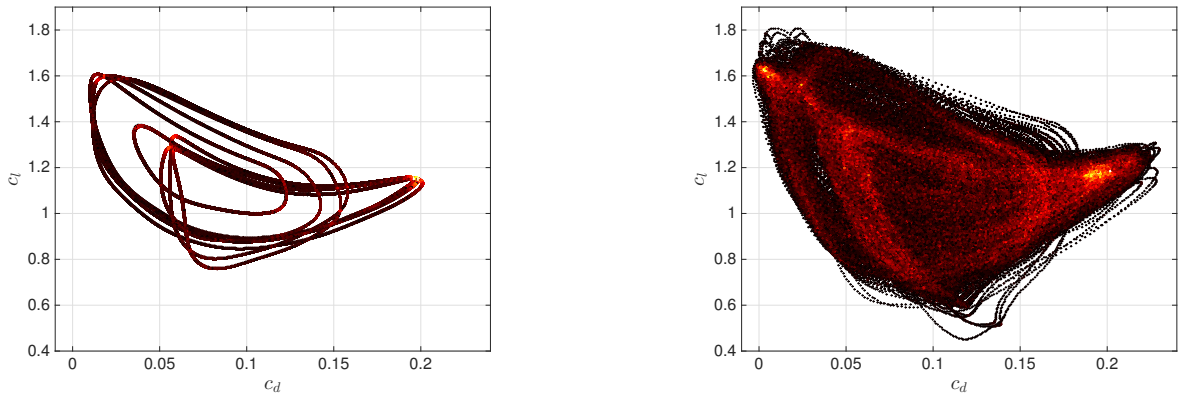

(a) Mesh No. 5

(b) Mesh No. 7

Figure 6: (c_d, c_l) trace over a time interval $20,000\ c/a_\infty$. The dots are colored by probability density function in (c_d, c_l) space.

computed with discrete systems that are much less chaotic than the underlying turbulent flow.

VI. Conclusions

We investigated the impact of the numerical discretization on the Lyapunov spectrum of the chaotic, separated flow around the NACA 0012 airfoil at a low Reynolds number. Numerical results showed that the time discretization has a small effect on the Lyapunov spectrum for the time-step sizes Δt typically used in CFD practice. In particular, the asymptotic spectrum as Δt for this wall-bounded flow was achieved with global CFL numbers $\mathcal{O}(10^1 - 10^2)$. The spatial discretization, however, was shown to dramatically change the dynamics of the system. First, the discretized system poorly reproduced the dynamics of the flow, and spurious dynamics were observed, below some spatial resolution threshold. Second, above this resolution threshold, the discrete system continued to become more and more chaotic even with finer meshes than the best practice for this type of flows. This indicates that the asymptotic Lyapunov spectrum as the mesh is refined is difficult to achieve in practice even for simple flows. Based on these results, we concluded the paper with a discussion on the feasibility of adjoint-based sensitivity analysis for chaotic flows.

Acknowledgements

The authors acknowledge AFOSR Award FA9550-15-1-0072 under Dr. Fariba Fahroo and Dr. Jeanluc Cambrier, Stanford CTR Summer Program 2016, and Dr. Patrick Blonigan.

References

[1]G. Benettin, L. Galgani, A. Giorgilli, J. Strelcyn, Lyapunov characteristic exponents for smooth dynamical systems and for Hamiltonian systems; a method for computing all of them. Part 2: Numerical application, Meccanica 15 (1) (1980) 21–30.

[2]P.J. Blonigan, Q. Wang, Multiple Shooting Shadowing for Sensitivity Analysis of Chaotic Systems and Turbulent fluid flow, In: 53rd AIAA Aerospace Sciences Meeting, Kissimmee, USA, Jan 2015.

[3]P.J. Blonigan, Q. Wang, E. Nielsen, B. Diskin, Least squares shadowing sensitivity analysis of chaotic flow around a two-dimensional airfoil, In: 54th AIAA Aerospace Sciences Meeting, San Diego, USA, Jan 2016.

[4]P.J. Blonigan, P. Fernandez, S.M. Murman, Q. Wang, G. Rigas, L. Magri, Towards a chaotic adjoint for LES, Proceedings of the Center for Turbulence Research Summer Program 2016, pp. 385–394, Jan 2017.

[5]N. Chandramoorthy, P. Fernandez, C. Talnikar, Q. Wang, The Ensemble Adjoint Method for Chaotic CFD: A Feasibility Study, In: 23rd AIAA Computational Fluid Dynamics Conference, Denver, USA, Jun 2017.

[6]N. Chandramoorthy, P. Fernandez, C. Talnikar, Q. Wang, On the rate of convergence of ensemble sensitivity estimators in chaotic dynamical systems, In consideration for submission to J. Comput. Phys.

[7]J.-P. Eckmann, D. Ruelle, Ergodic theory of chaos and strange attractors, Rev. Mod. Phys. 57 (3) (1985) 617–656.

[8]P. Fernandez, N.C. Nguyen, X. Roca, J. Peraire, Implicit large-eddy simulation of compressible flows using the Interior Embedded

Discontinuous Galerkin method, In: 54th AIAA Aerospace Sciences Meeting, San Diego, USA, Jan 2016.

[9]P. Fernandez, High-Order Implicit-Large Eddy Simulation for Transitional Aerodynamic Flows, Master Thesis, Department of Aeronautics and Astronautics, Massachusetts Institute of Technology, 2016.

[10]P. Fernandez, N.C. Nguyen, J. Peraire, The hybridized Discontinuous Galerkin method for Implicit Large-Eddy Simulation of transitional turbulent flows, J. Comput. Phys. 336 (1) 308–329, 2017.

[11]P. Fernandez, Q. Wang, Lyapunov spectrum of the separated flow around the NACA 0012 airfoil and its dependence on numerical discretization, J. Comput. Phys., Accepted for publication.

[12]H. Haken, At least one Lyapunov exponent vanishes if the trajectory of an attractor does not contain a fixed point, Phys. Lett. A 94 (2) (1983) 71–72.

[13]L. Keefe, P. Moin, J. Kim, The dimension of attractors underlying periodic turbulent Poiseuille flow, J. Fluid Mech. 242 (1992) 1–29.

[14]D.J. Lea, M.R. Allen, T.W. Haine, Sensitivity analysis of the climate of a chaotic system, Tellus A 52 (2000) 523–532.

[15]C.E. Leith, Climate Response and Fluctuation Dissipation, J. Atmos. Sci. 32 (1975) 2022–2026.

[16]G. Nastac, J. Labahn, L. Magri, M. Ihme, Lyapunov Exponent as a Metric for Assessing the Dynamic Content and Predictability of Large-Eddy Simulations, Phys. Rev. Fluids, Under Review.

[17]A. Ni, Q. Wang, Sensitivity analysis on chaotic dynamical system by Non-Intrusive Least Square Shadowing (NILSS), J. Comput. Phys., Under review, arXiv: 1611.00880.

[18]E. Özkaya, N.R. Gauger, A. Nemili, Chaotic Behavior of Stiff ODEs and Their Derivatives: An Illustrative Example, arXiv:1610.03358.

[19]V.I. Oseledets, Multiplicative ergodic theorem: Characteristic Lyapunov exponents of dynamical systems, Trudy MMO 19 (1968) 179–210.

[20]T. Pulliam, J. Vastano, Transition to chaos in an open unforced 2D flow, J. Comput. Phys. 105 (1993) 133–149.

[21]L. Sirovich, A. Deane, A computational study of Rayleigh-Benard convection. Part 2. Dimension considerations, J. Fluid Mech. 222 (1991) 251–266.

[22]K.A. Takeuchi, H-l Yang, F. Ginelli, G. Radons, H. Chaté, Hyperbolic decoupling of tangent space and effective dimension of dissipative systems, Phys. Rev. E 84 (2011) 046214.

[23]J. Thuburn, Climate sensitivities via a Fokker-Planck adjoint approach, Q. J. Roy. Meteor. Soc. 131 (605) (2005) 73–92.

[24]S. Vannitsem, C. Nicolis, Lyapunov vectors and error growth patterns in a T21L3 quasigeostrophic model, J. Atmos. Sci. 54 (1997) 357–361.

[25]J.A. Vastano, R.D. Moser, Short-time Lyapunov exponent analysis and the transition to chaos in Taylor-Couette flow, J. Fluid Mech. 233 (1991) 83–118.

[26]Q. Wang, R. Hui, P. Blonigan, Least squares shadowing sensitivity analysis of chaotic limit cycle oscillations, J. Comput. Phys. 267 (2014) 210–224.

[27]M. Wei, J.S. Frederiksen, Error growth and dynamical vectors during southern hemisphere blocking, Nonlinear Processes Geoph. 11 (2004) 99–118.

[28]M. Xu, M.R. Paul, Covariant Lyapunov vectors of chaotic Rayleigh-Bénard convection, Phys. Rev. E 93 (2016) 062208.